



This is a repository copy of *Regulating the formation and extent of crazing through the application of argon plasma surface functionalisation*.

White Rose Research Online URL for this paper:

<https://eprints.whiterose.ac.uk/204475/>

Version: Published Version

Article:

Farr, N.T.H. orcid.org/0000-0001-6761-3600 (2023) Regulating the formation and extent of crazing through the application of argon plasma surface functionalisation. *Polymer Testing*, 128. 108244. ISSN 0142-9418

<https://doi.org/10.1016/j.polymertesting.2023.108244>

Reuse

This article is distributed under the terms of the Creative Commons Attribution (CC BY) licence. This licence allows you to distribute, remix, tweak, and build upon the work, even commercially, as long as you credit the authors for the original work. More information and the full terms of the licence here:

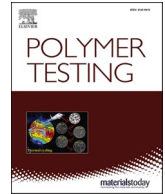
<https://creativecommons.org/licenses/>

Takedown

If you consider content in White Rose Research Online to be in breach of UK law, please notify us by emailing eprints@whiterose.ac.uk including the URL of the record and the reason for the withdrawal request.



eprints@whiterose.ac.uk
<https://eprints.whiterose.ac.uk/>



Regulating the formation and extent of crazing through the application of argon plasma surface functionalisation

Nicholas T.H. Farr^{a,b,*}

^a Department of Materials Science and Engineering, University of Sheffield, Sir Robert Hadfield Building, Mappin Street, UK

^b Insigneo Institute for in silico Medicine, The Pam Liversidge Building, Sir Robert Hadfield Building, Mappin Street, Sheffield, UK

ARTICLE INFO

Keywords:

Crazing
Polymer processing
Argon plasma
Polymer testing
Mechanochemistry

ABSTRACT

Polymer crazing is a phenomenon observable as fine cracks on the surface of a material. For polymers crazing is often a precursor to mechanical failure with the capacity of a craze to propagate and develop into a larger structural crack. In this study polypropylene (PP) fibres, known to be susceptible to crazing, were subjected to argon (Ar) plasma treatment with the aim of creating a crosslinked surface that displays the ability to withstand the formation of crazes. To evaluate Ar plasma success at achieving this aim: the resulting Ar treated fibres were characterised to evaluate their capacity to avoid the formation of crazes and also identify any changes induced to the chemical and mechanical properties of PP as a consequence of Ar plasma exposure. This analysis was conducted by application of low voltage (LV)-scanning electron microscopy imaging, uniaxial tensile testing, Energy Dispersive X-ray Spectroscopy (EDS) and attenuated total reflectance - fourier-transform infrared spectroscopy (ATR-FTIR). The results of this study highlight the potential of the application of Ar plasma to influence the formation of crazes on PP fibres after exposure to repeated dynamic distention cycles. Ar plasma treated PP also showed a capacity to reduce bulk fibre oxidation when compared to that of non-treated PP when exposed to dynamic distention and subsequently immersed in an oxidative stress environment.

1. Introduction

Materials are rarely deployed in static environments, rather they are regularly exposed to diverse and varying stresses within dynamic environments. These stresses, initially effecting the surface of materials, can have detrimental consequences to key functional material properties. This includes the formation of crazes, a precursor to a deeper crack, which has been associated as a prime failure mechanism for polyolefines [1]. Crazes have been extensively studied with their origins known to originate from high tensile and bending stresses [2,3]. Crazes often represent the first step of the fracture process in polymers in relation to the characteristic ratio of the intrinsic flexibility and rigidity of a molecular chains [4]. The void space which crazes create introduce inhomogeneities in the polymer surface which if not stabilised, by fibril polymer chains, can break and effect bulk fibre structural mechanical properties. Crazes are most common in fibrous structured polymers where the stress distribution is favourable for their formation through fibrillar deformation [5].

Aside from being a precursor to a crack, with potential for fibre breakage and failure, crazes have been considered to act as a route for

oxidation to occur within the bulk polymer fibres. Recently emphasised has been the effect of crazes on the functional properties of surgical mesh fabricated from polypropylene (PP) fibres [6]. Safety concerns have long been raised regarding PP mesh implants as a consequence of the findings of research examining both patient outcomes and *in vitro* studies [7]. Studies have also long reported surface alterations, such as cracks and flaking, on explanted PP mesh [8,9]. With explanted PP meshes from humans having shown the occurrence of crazing on the surfaces of fibres [10]. The combination of dynamic distention and oxidative stress has shown the capacity to cause bulk fibre oxidation, with the formation of crazes considered as a pathway for oxidative agents. For PP fibres, studies have shown that dynamic distention of PP mesh materials for just 3 days causes irreversible distortion and remodelling of the mechanical properties of PP meshes [11]. This is not surprising with mechanical energy known to have the ability to break and form chemical bonds with the capacity to effect bulk mechanical properties [12,13]. It has been well documented that crazing can both reduce the ductility of a polymer under tensile loads and form shear stress bands which under compression lead to structural deformation [14].

* Department of Materials Science and Engineering, University of Sheffield, Sir Robert Hadfield Building, Mappin Street, UK.

E-mail address: n.t.farr@sheffield.ac.uk.

<https://doi.org/10.1016/j.polymeresting.2023.108244>

Received 1 September 2023; Received in revised form 10 October 2023; Accepted 17 October 2023

Available online 17 October 2023

0142-9418/© 2023 The Author. Published by Elsevier Ltd. This is an open access article under the CC BY license (<http://creativecommons.org/licenses/by/4.0/>).

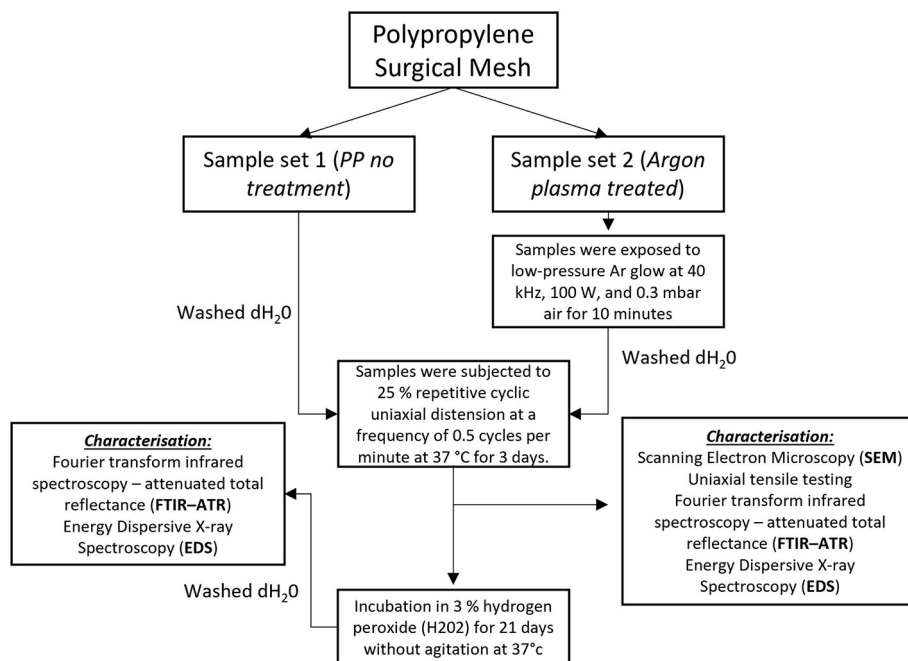


Fig. 1. Workflow of the experimental set up.

The ability to tailor or mediate the formation of crazes is an attractive proposition and one that could greatly improve current polymer processing. It has been proposed that crazing can be avoided by the modification of polymer chain structures. Specifically, through increasing the number of entangled molecular chains which span the crazes fracture interface [1]. It has been considered that increasing a materials molecular entanglement may reduce the craze propagation criterion thereby reducing the likelihood that formation of larger fracture sites will occur. It is expected that this would result in minimising the effects of repeated dynamic distention and reduce the capacity of bulk fibre oxidation. The latter being as a response to the reduction of crazes restricting a pathway for bulk fibre oxidation. With the aim to minimise craze formation this study applies low-pressure argon (Ar) plasma to PP fibre mesh to generate a crosslinked “sheath” within the fibre surface to reduce the potential for surface crazing. For polymer processing, Ar plasma has been previously shown not to impart functional group subsurface alterations [15] but has the capacity to create highly cross-linked surfaces [16] and nano-surface structures [17]. Despite Ar plasma known to facilitate cross-linking via fragmentation and subsequent recombination of polymer chains [18–20], no study to date has applied Ar plasma with the objective of deterring craze formation. To evaluate if the Ar plasma treatment reduced the formation of crazes in PP samples low voltage – scanning electron microscopy (LV-SEM) was performed, and to observe if the treatment mitigated the effects of dynamic distention or accelerated oxidation, uniaxial tensile testing, energy dispersive X-ray spectroscopy (EDS) and attenuated total reflectance - Fourier-transform infrared spectroscopy (ATR-FTIR) was performed.

2. Materials and methods

A workflow of the experimental set up is presented in Fig. 1.

2.1. Sample preparation

Strips of commercially available PP surgical mesh, (Prolene® Mesh, Ethicon, Belgium), were cut into 1.5 cm × 1.5 cm strips using sterilised scissors within a cell culture cabinet along the longitudinal direction of the surgical mesh. The mesh selected for this study was a monofilament

textile knitted material with a macroporous structure and a fibre diameter of ~150 µm.

2.1.1. Low temperature argon (Ar) plasma treatment

A subset of samples were prepared by exposing them to low-pressure Ar glow discharge in a Diener Electronic Zepto plasma cleaner at 40 kHz, 100 W, and 0.3 mbar air for 10 min in Tyvek gas semi-permeable packaging. 10 min of exposure was chosen as a maximum limit to exclude any effects of sample heating which have been shown to lead to additional surface modifications [21].

2.1.2. Dynamic distention

The application of *in vitro* fatigue testing to assess surgical mesh has been published in detail previously [11]. In brief, both Ar plasma treated, and control PP samples were clamped flat with a distance of 8 mm between the two grips of a TC-3 load bioreactor (Ebers Medical Technology SL, Zaragoza, Spain) along the longitudinal direction of the surgical mesh. Samples were immersed in deionised water. Samples were subjected to 25 % repetitive cyclic uniaxial distention at a frequency of 0.5 cycles per minute at 37 °C for 3 days.

2.1.3. Accelerated degradation test

Samples were subject to an accelerated degradation test. The procedures adopted for the study were conducted in accordance with the recommendations of ISO 10993-13, Biological Evaluation of Medical Devices—Part 13: Identification and Quantification of Degradation Products from Polymeric Medical Devices [22]. For both test conditions 10 g of mesh was placed in the stainless steel collection chamber with an appropriate (test article solution ratio of 1 g:10 mL) of 3% hydrogen peroxide (H₂O₂) Hydrogen peroxide solution, contains inhibitor, 30 wt % in H₂O, ACS reagent. (Sigma-Aldrich, UK). Samples were then incubated at 37 °C for 21 days without agitation. Both temperature and the time duration selected where selected as a result of reference to ISO standards and previous studies [8,22].

2.2. Low voltage (LV)-scanning electron microscopy imaging

FEI Helios Nanolab G3 (FEI Company, US) and Helios G4 DualBeam (ThermoFisher Scientific, US) microscopes were employed for surface

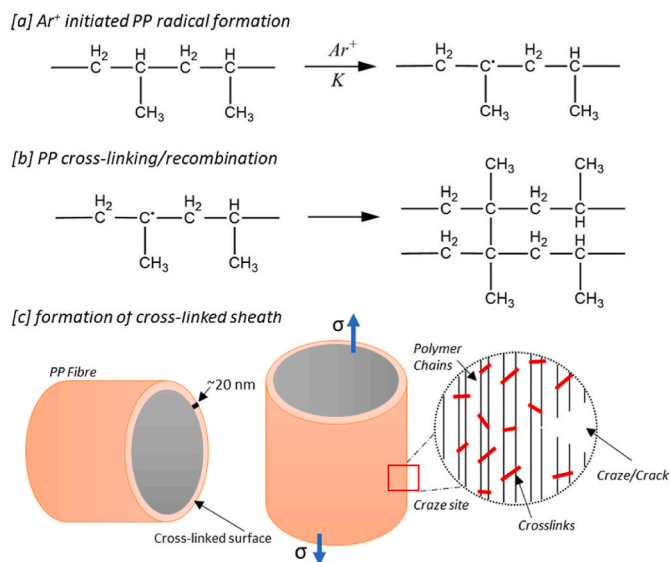


Fig. 2. [a] Reaction of argon plasma initiating PP free radical formation. [b] PP recombination reaction. [c] hypothesised formation of PP crosslinked surface sheath.

morphology observations of PP samples. In contrast to common scanning electron microscopy (SEM) analysis practice, samples were not pre-treated with a conductive coating by deposition. An accelerating voltage of 1–2 keV at typical chamber vacuum pressures in the range of 10^{-6} mbar and a working distance of 4 mm were chosen to avoid sample damage through surface charging. An Everhart-Thornley Detector (ETD) was selected for low magnification SE images and a Through Lens Detector (TLD) for high magnification SE images.

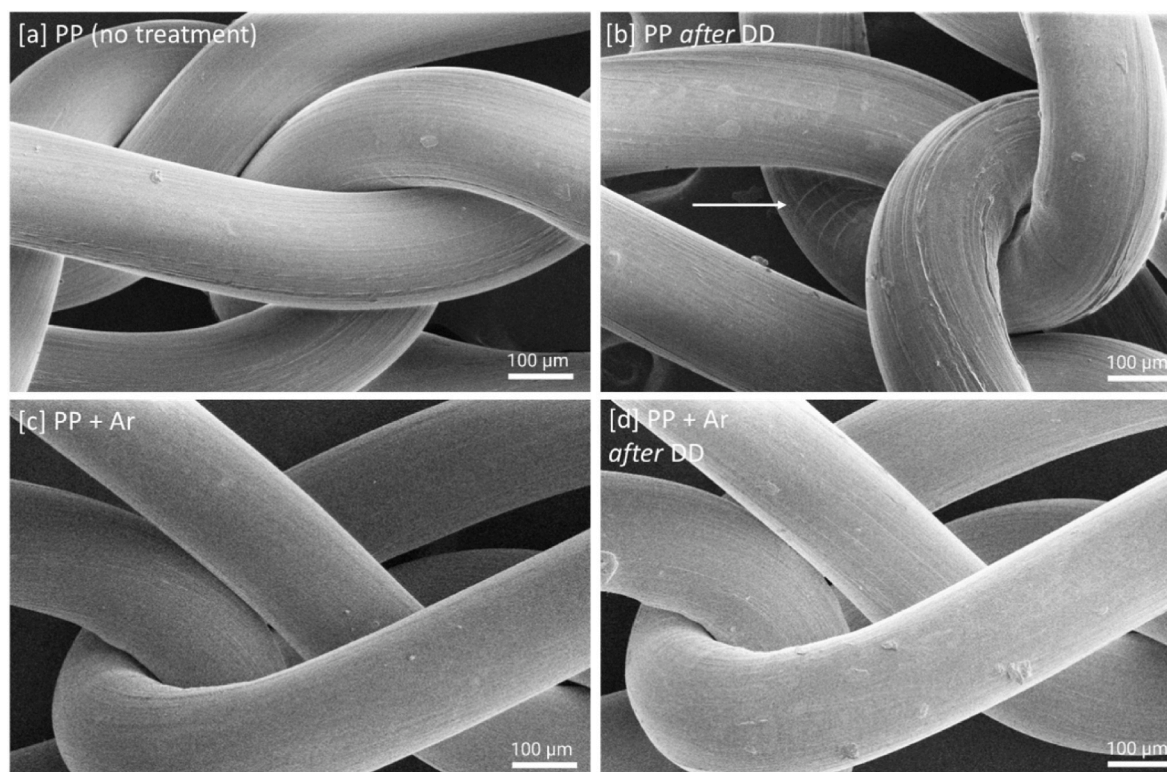


Fig. 3. LV-SEM images of [a] non-treated PP, [b] non-treated PP after dynamic distention (DD), [c] Ar plasma treated PP, [d] Ar plasma treated PP after dynamic distention.

2.3. Uniaxial tensile testing

Uniaxial ramp testing was performed for both PP sample sets after dynamic distention conditions. A tensiometer (MultiTest-dV, Mecmesin) was used. Test pieces ($n = 4$, for each material) were clamped between two grips of the tensiometer with a testing length of 10 mm. A load cell of 250 N was used. The sample meshes test pieces were loaded in the longitudinal direction, in the direction of use as indicated by the manufacturer. A tensile test was then applied at a rate of 0.1 mm s^{-1} . All experiments were performed under constant laboratory conditions ($23 \text{ }^\circ\text{C}$, British air humidity 80 %).

2.4. Energy dispersive X-ray spectroscopy

FEI Nova nanoSEM 450 (FEI Company, USA) SEM equipped with an Energy Dispersive X-ray Spectroscopy (EDS) detector (Oxford Instruments, UK) was used to capture EDS spectra. EDS spectra were taken from the centre of each PP fibre to mitigate any effects associated with fibre orientation. The spectra were obtained with a 10 keV accelerating voltage using a 4.5 spot probe current at a working distance of 5 mm. Data analysis was automated by the application of Aztec EDS analysis software (Oxford Instruments, UK).

2.5. Attenuated total reflectance - fourier-transform infrared spectroscopy (ATR-FTIR)

Infrared spectra were obtained for all test PP samples with a NICO-LET 380 Fourier-transform infrared (FTIR) spectrometer (ThermoFisher Scientific, US). Samples were purged with dry air before spectra collection in the range from 500 to 4000 cm^{-1} averaging 32 scans and a resolution of 4 cm^{-1} . The samples were analysed in their solid state form using an attenuated total reflection (ATR) accessory with a Golden Gate® diamond crystal (Specac, UK).

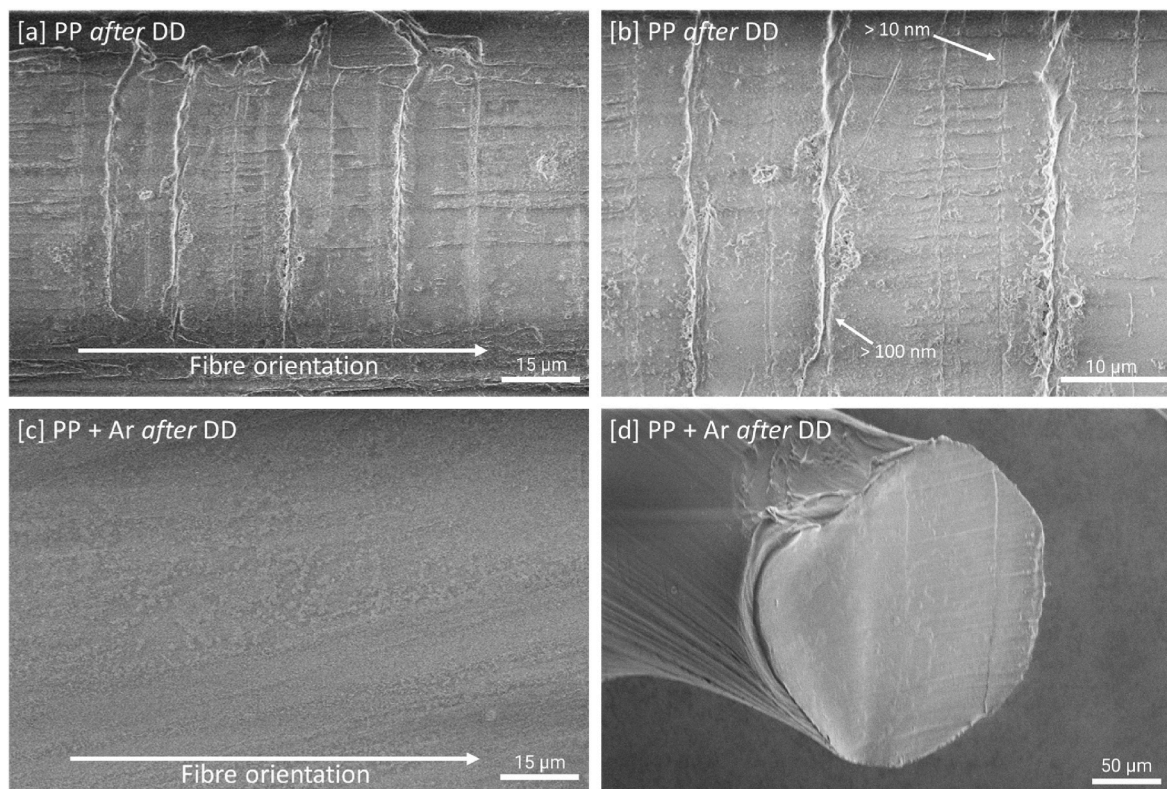


Fig. 4. LV-SEM images of [a-b] non-treated PP after dynamic distention (DD). [c] Ar plasma treated PP after dynamic distention and [d] a cryo cross-section of a Ar plasma treated PP after dynamic distention.

2.6. Statistical analysis

Statistical analysis and graph production was performed using the GraphPad Prism version 9 software (GraphPad Software, Inc.; La Jolla, USA). Data are reported as mean \pm standard deviation. The significance level was defined as $p < 0.05$.

3. Results and discussion

3.1. Experimental underpinning and theoretical hypothesis

It has been long established that various different types of plasma treatments; gas compositions and plasma conditions can impart varying surface modifications on polymers [15–20,23]. Surface modifications including both physical (etching/roughness) and chemical (addition of surface functional groups/crosslinking) have been employed for the benefit of processing polymers. However, to date there has been little to no consideration given to the application of plasma for the use of reducing the capacity of a fibrous polymers to undergo the process of crazing. The design of this study set on the application of Ar plasma to create a crosslinked surface layer on the surface of PP to not only reduce the formation of crazes but to restrict the route of bulk fibre oxidation provided by its propagation pathway. Fig. 2A presents the known mechanism by which Ar plasma can be applied to initiate PP radical formation by creating initial chain fragmentation (note this is a simplified reaction and within the molecular structure of PP it is expected that there would be non-linear oriented polymer chains with entanglements present). Fig. 2B presents how the creation of free radicals can then trigger a recombination reaction creating crosslinked PP polymer chains. It is the hypothesis of this study that the formation of such crosslinked changes will increase the molecular chain entanglement localised to the surface of the PP fibres. It has previously been considered that increasing the molecular chain entanglement of a

polymers surface could in practice reduce the capacity of crazes to form. As presented in Fig. 2C the expectation is that the increase in crosslinks (creation of a surface sheath) will reduce the propagation of surface crazes when mechanical stress is applied to the polymer.

To test the hypothesis, PP fibres after Ar plasma treatment underwent dynamic distention, shown previously to produce crazes [6]. The PP fibres were then characterised to evaluate if crazes were identifiable and also if changes to the PP material properties known to be of a consequence of craze formation, eg fibre stiffness and oxidation, were observable. Additionally, recent studies have hypothesised the capacity of crazing to allow for a pathway for bulk fibre oxidation [6,24]. To test if crazing could provide such a pathway, accelerated degradation after dynamic distention was performed on PP fibres pre and post Ar plasma treatment to give insights into potential routes of fibre oxidation.

3.2. Surface morphology

Fig. 3 presents LV-SEM images of PP mesh with and without Ar treatment and before and after dynamic distention. Regardless of the PP mesh undergoing no treatment (Fig. 3A), surface markings are present on PP fibres when imaged prior to dynamic distention. These markings are observable longitudinally and considered to be due to mechanical stress applied in the fabrication of the mesh knit structures. After dynamic distention it is notable that non-treated fibres (Fig. 3B) exhibit cracking not only along the longitudinal markings observed prior to dynamic distention, but also craze related cracking (highlighted by white arrow in (Fig. 3B)) across the fibres. For images collected from PP + Ar before dynamic distention (Fig. 3C) the surface morphology appears very similar to that of non-treated PP (Fig. 3A). Minor differences are observable however, notably in the reduction of the size of particles apparent on non-treated fibre surfaces. It appears the application of Ar treatment has etched away at these surface particles. This is observation consistent with known mechanisms of Ar plasma applications [25]. After

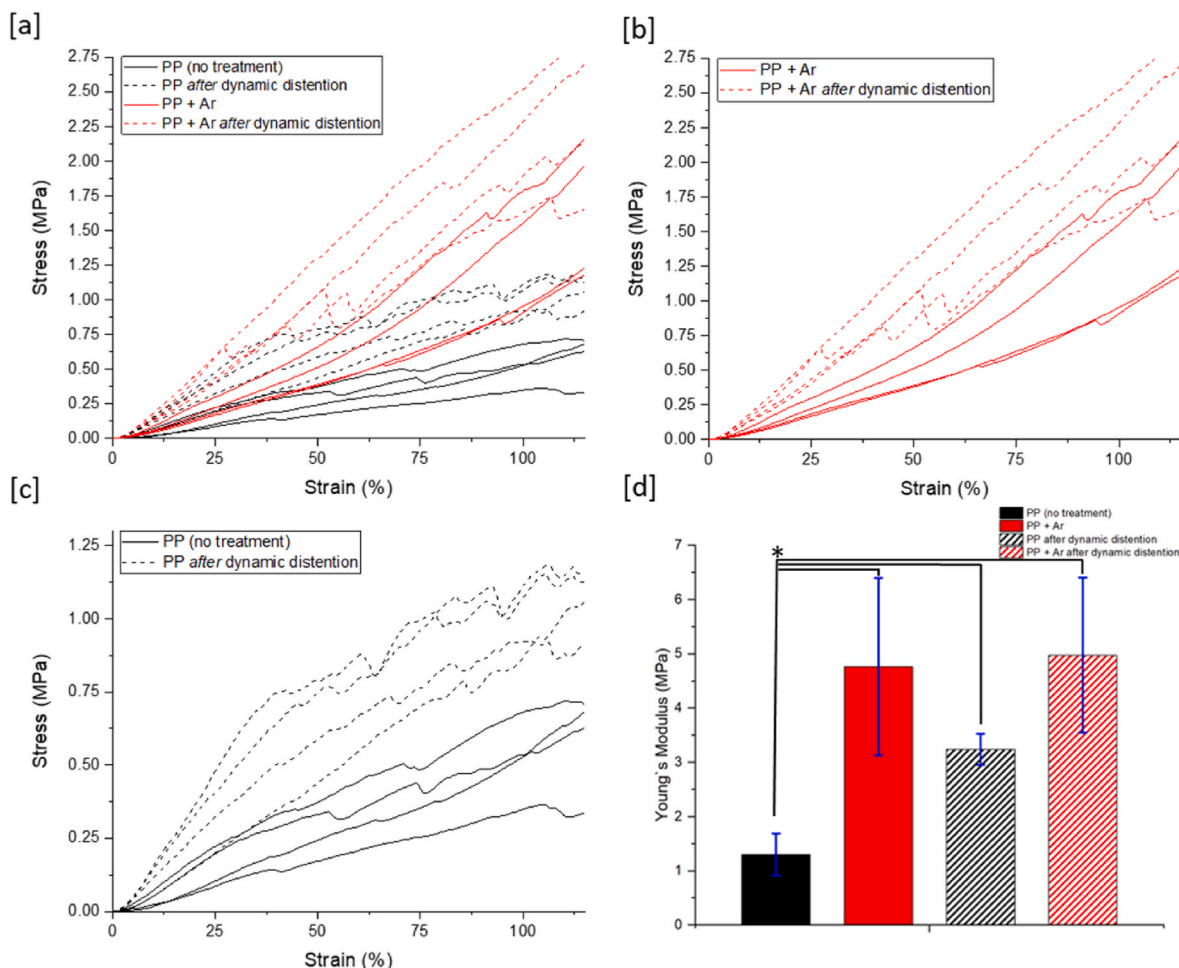


Fig. 5. [a-c] Stress-strain curves of PP mesh with and without Ar plasma treatment and after dynamic distention ($n = 4$). [d] Graph presenting the Young's modulus of PP mesh with and without Ar plasma treatment and after dynamic distention [$n = 4$] (* $p < 0.05$ significance).

dynamic distention the PP + Ar fibres appear to display less surface cracking and markings compared to that of non-treated PP. Additionally unlike PP after dynamic distention, there also appears to be no apparent signs of surface crazing, however surface aberration markings are still observable.

To better visualise the surface morphology of PP fibres after dynamic distention, LV-SEM images at higher magnifications using a through-lens-detector (TLD) were collected and presented in Fig. 4 (A-C). Without the application of Ar plasma treatment, and as published in previous studies, it is observable that after dynamic distention PP undergoes crazing (Fig. 4A&B) [6]. In this study it is observable that crazing occurs both in the micron and nanoscale length scale (Fig. 4B), with larger crazes having the potential to propagate into more conventional cracks with a void. When comparing the surface morphology of PP with and without Ar plasma treatment after dynamic distention (Fig. 4. A&C) aside from the reduction of crazes it is observable other visual differences exist. For PP treated with Ar plasma it is apparent that nanoscale "islands" are present along the fibres. These islands of nanoparticles are expected to be formed during plasma etching. It is proposed that during the Ar plasma interaction with the PP surface, amorphous regions are etched away [16,26]. During a high energy physical etching process, which has previous been employed to nanotexture amorphous carbon films [26], free radicals can then trigger a recombination reaction creating crosslinked polymer chains [15,16]. It is considered that this also creates a plasma-initiated fibre coating/sheath with an increased crosslinking density. Fig. 4 D displays an image of a cross-sectioned Ar treated PP fibre with what appears to be a sheath-like

coating peeling away from the fibre bulk after cyro-sectioning.

3.3. Uniaxial tensile testing

The tensile properties of PP mesh after dynamic distention, both with and without Ar plasma treatment was measured using a tensiometer and comparisons made to control (with no dynamic distention) samples. Stress strain curves are displayed in Fig. 5A-C and bulk mechanical properties (Fig. 5D) are presented showing both mesh materials were affected by dynamic distention. This result is consistent with previously published studies which have shown the impact of repeated dynamic distention of PP mesh [6,11]. Comparing both Ar treated and control PP mesh after no dynamic distention it is notable that the application of Ar plasma treatment increased the stiffness and subsequent Young's Modulus on the PP mesh fibres. This again is an expected result as it has been shown Ar plasma treatment has the capacity to not only increase the density of polymer crosslinks but also directly affect a polymers surface stiffness [15,16]. It is therefore considered that the surface stiffness and increased crosslink density are directly associated rather than separate phenomena.

When comparing Ar plasma treated samples (with and without dynamic distention) (Fig. 5B) with non-treated PP (without dynamic distention) (Fig. 5C) it is notable that there is a larger increase in stiffness and subsequent Young's Modulus for non-treated PP samples. Unlike non-treated PP, for Ar plasma treated samples there is no significant increase in Young's Modulus between with and without dynamic distention. This is of note as previous studies have indicated that crazing

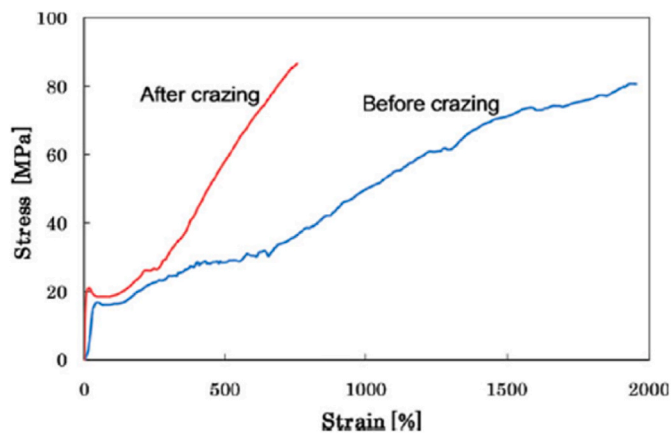


Fig. 6. Reproduced with permission from Ref. [3] under <https://creativecommons.org/licenses/by/3.0/> "Stress-strain curves of the PP filament: (a) The unprocessed filament and (b) the crazed filament."

alone leads to increased crystallinity and stiffness [Fig. 6] [3]. Taking into consideration that the Ar plasma treatment initially effected the mechanical properties of the PP fibres it can be concluded that dynamic distention effected the bulk individual fibres, less than that of the non-treated PP. This result does not indicate Ar plasma treated would be a more suitable material for use as a surgical mesh, as increased stiffness

may not be a desirable trait, but instead that the use of Ar plasma can alter the effect dynamic distention/formation of crazes has on the mechanical properties of PP fibres as hypothesised.

3.4. Quantification of sub-surface chemistry by ATR-FTIR and EDS

To obtain a measure of sub-surface oxidation for Ar plasma treated and control PP meshes, ATR-FTIR was performed (providing ~2 μm sampling depth). Fig. 7A presents the ATR-FTIR spectra obtained from a control PP mesh sample and all test samples. FTIR spectra of non-treated PP (A.i), PP after Dynamic distention (A.ii), PP + Ar plasma treatment (A.iii) and PP + Ar plasma treatment after dynamic distention (A.iv) showed no pronounced carbonyl (C=O; expected range: 1750-1500 cm⁻¹) or hydroxyl (-OH; expected range 3600-3000 cm⁻¹) groups [27, 28]. This indicates that neither dynamic distention nor Ar plasma treatment, alone or combined, imparted any notable difference to the sub-surface chemistry of PP. This is not an unexpected result as it is known the Ar plasma penetrates in the order of nanometers into a polymers surface making subsurface interactions at the micron scale identifiable by ATR-FTIR unattainable.

It has previously been stated that crazing of the PP is due to two factors *in vitro*: tensile forces and chemical degradation of the material by oxidizing substances. Both factors reinforce each other. The first cracks in the material create a new contact surface for oxidizing agents, which can then penetrate faster and deeper into the material and further weaken its strength. Thus, such a combined mechanism has the potential

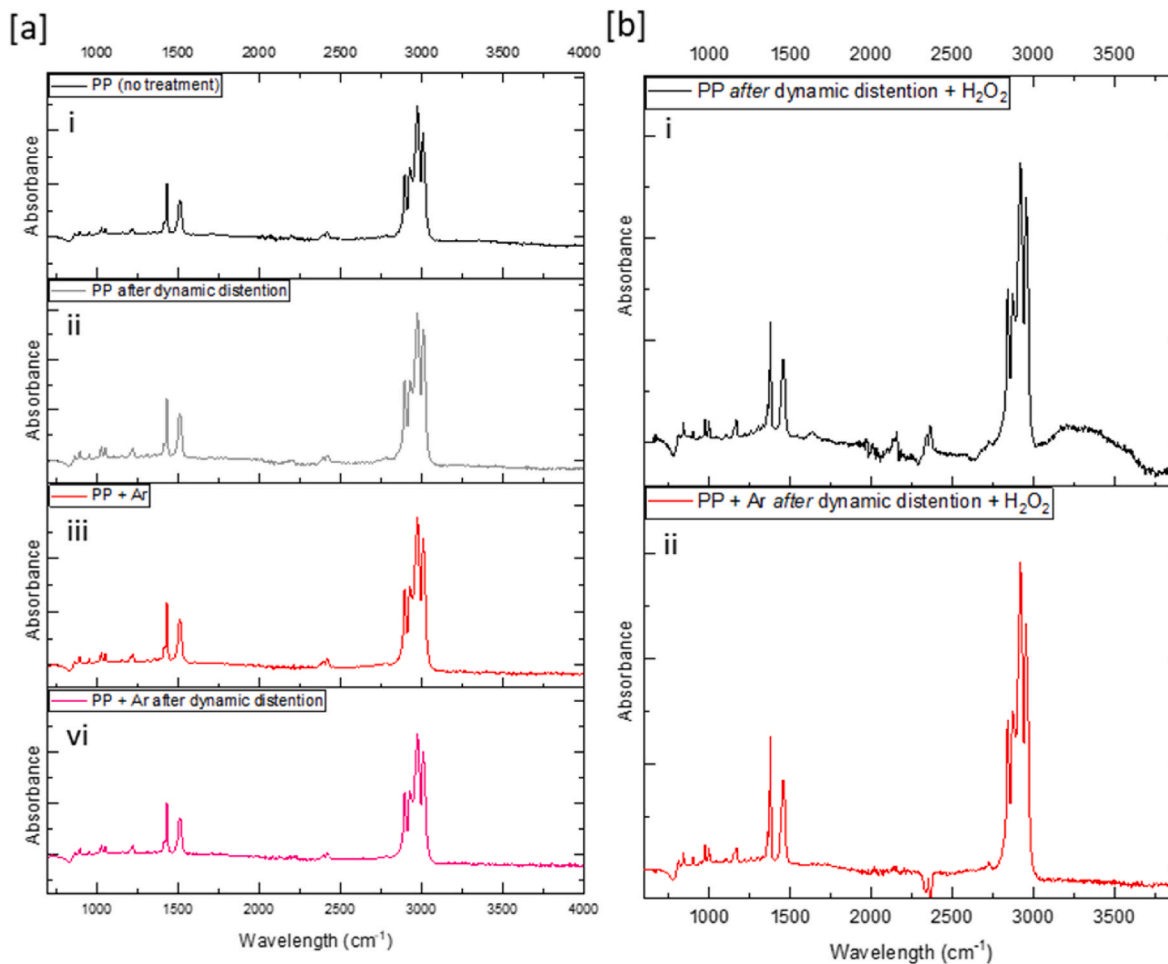


Fig. 7. [a] ATR-FTIR spectra collected from non-treated PP; non-treated PP after dynamic distention; Ar plasma treated PP; Ar plasma treated PP after dynamic distention. [b] ATR-FTIR spectra collected from non-treated PP (after dynamic distention and H₂O₂ exposure) and Ar plasma treated PP (after dynamic distention and H₂O₂ exposure).

to be a significant driver of fibre failure. Consequently, Fig. 7B presents FTIR spectra of Ar plasma treated and non-treatment PP after dynamic distention and acceleration degradation. Compared to the Ar treated PP, the non-treated PP showed a significant increase in both C=O and OH groups. These results indicate, as previously shown, that the combined approach of dynamic distention and oxidative stress can cause bulk fibre oxidation. Of specific interest is that no such oxidation peaks were observable within the Ar treated PP. To confirm these findings EDS was performed on non-treated PP and Ar treated fibres after both dynamic distention and accelerated degradation. EDS has previously been applied to identify oxidation of PP explanted from patients [29]. EDS spectra presented in Fig. S1 (supporting information) displays peaks related to Carbon and Oxygen which was found present in both samples, however the ratio of oxygen to carbon notably reduced within the Ar treated PP sample. Results provided from both ATR-FTIR and EDS indicate that the crosslinked surface modification on the Ar treated PP fibres was sufficient to restrict the process of bulk fibre oxidation. This result indicates that decreasing the capacity of crazes to form can influence the route to fibre oxidation. Previous studies have shown that PP has the capacity to oxidise in response to oxidative and mechanical stress, termed “mechanochemical stress” [6]. Through the application of Ar plasma this study has provided evidence that it is possible to modulate this response.

4. Conclusions

The results presented in this study show that Ar plasma treatment has the capacity to form a crosslinked layer on the surface of PP. This crosslinked layer increases the surface localised molecular chain entanglement and decreases the formation of crazes. The reduction of crazes is shown to not only reduce the observable changes to fibre stiffness post dynamic distention, but also can reduce the effect of mechanochemical stress that is a cause of bulk fibre oxidation. The results from this study provides insights into how the application of plasma to produce surface coatings could be optimized in future studies to produce polymeric fibres less susceptible to the effects of crazing.

Author statement

NTHF: Conceptualization; Data curation; Formal analysis; Funding acquisition; Investigation; Methodology; Resources; Project administration; Software; Supervision; Validation; Funding acquisition; Visualization; Roles/Writing – original draft; Writing – review & editing.

Declaration of competing interest

The author declares no known competing financial interests or personal relationships that could have appeared to influence the work reported in this paper.

Data availability

Data will be made available on request.

Acknowledgements

N.T.H.F acknowledges the Sorby Centre for Electron Microscopy at

the University of Sheffield for allowing electron microscopy and analysis to be performed. Funding: This work was supported by Engineering and Physical Sciences Research Council (EPSRC) [EP/T517835/1, EP/V012126/1].

Appendix A. Supplementary data

Supplementary data to this article can be found online at <https://doi.org/10.1016/j.polymertesting.2023.108244>.

References

- [1] R.A.C. Deblieck, D.J.M. van Beek, K. Remerie, I.M. Ward, *Polymer* 52 (2011) 2979–2990, <https://doi.org/10.1016/j.polymer.2011.03.055>.
- [2] Emile S. Greenhalgh (Ed.), *Delamination-dominated Failures in Polymer Composites*, Woodhead Publishing, 2009, pp. 164–237.
- [3] A. Takeno, M. Miwa, T. Yokoi, K. Naito, A.A. Merati, *J. Appl. Polym. Sci.* 128: 3564–3569. <https://doi.org/10.1002/app.38485>.
- [4] S. Wu, *J. Polym. Sci., Part B: Polym. Phys.* 27 (1989) 723.
- [5] E. Passaglia, *J. Phys. Chem. Solid.* 48 (11) (1987) 1075–1100.
- [6] N.T.H. Farr, S. Roman, J. Schäfer, A. Quade, D. Lester, V. Hearnden, S. MacNeil, C. Rodenburg, *RSC Adv.* 11 (55) (2021) 34710–34723.
- [7] P. Dallenbach, *Int J Womens Health* 7 (2015) 331–343.
- [8] N.T.H. Farr, C. Rauer, A.J. Knight, A.I. Tartakovskii, K.V. Thomas, *Nano Select* 4 (6) (2023) 395–407.
- [9] A. Imel, T. Malmgren, M. Dadmun, S. Gido, J. Mays, *Biomaterials* 73 (2015) 131.
- [10] V.V. Iakovlev, S.A. Guelcher, R. Bendavid, J. Biomed. Mater. Res. B Appl. Biomater. 105 (2) (2017) 237–248.
- [11] S. Roman, N. Mangir, L. Hympanova, C.R. Chapple, J. Deprest, S. MacNeil, *NeuroUrol. Urodyn.* 38 (2019) 107.
- [12] F. Verstraeten, R. Gostl, R.P. Sijbesma, *Chem. Commun.* 52 (2016) 8608–8611.
- [13] V.I. Vettegren, A.E. Tshmel, *Eur. Polym. J.* 12 (1976) 853.
- [14] T. Eliades, S. Zinelis, D.G. Kim, W.A. Brantley, *Structure/property relationships in orthodontic polymers*, in: Eliades, Theodore; Brantley, William A. *Orthodontic Applications of Biomaterials: a Clinical Guide*, Elsevier, Woodhead, 2017, pp. 39–59.
- [15] A. Sikora, D. Czyłkowski, B. Hrycak, M. Moczala-Dusanowska, M. Łapiński, M. Dors, M. Jasiński, *Sci. Rep.* 11 (2021), 9270, <https://doi.org/10.1038/s41598-021-88553-5>.
- [16] N. Farr, J. Thanarak, J. Schäfer, A. Quade, F. Claeysens, N. Green, C. Rodenburg, *Adv. Sci.* 8 (4) (2021).
- [17] A. Zaitsev, A. Lacoste, F. Poncin-Epaillard, A. Bès, D. Debarnot, *Surface and Coatings Technology*, vol. 330, 2017, pp. 196–203.
- [18] P. Weiss, *J. Polym. Sci., Polym. Lett. Ed.* 13 (3) (1975) 185–186.
- [19] V. Luque-Agudo, M. Hierro-Oliva, A.M. Gallardo-Moreno, M. González-Martín, *Polym. Test.* 96 (2021), 107097.
- [20] S. Vallon, B. Drévilion, F. Poncin-Epaillard, *Appl. Surf. Sci.* 108 (1) (1997) 177–185.
- [21] J. Yip, K. Chan, K.M. Sin, K.S. Lau, *Mater. Res. Innovat.* 6 (44) (2002) 4.
- [22] ISO 10993-13, *Biological Evaluation of Medical Devices—Part 13: Identification and Quantification of Degradation Products from Polymeric Medical Devices*.
- [23] D. Hegemann, H. Brunner, C. Oehr, *Nuclear Instruments and Methods in Physics Research Section B: Beam Interactions with Materials and Atoms*, vol. 208, 2003, pp. 281–286.
- [24] N.T.H. Farr, B. Klosterhalfen, G.K. Noé, *J. Biomed. Mater. Res. B Appl. Biomater.* 111 (5) (2023) 1142–1152.
- [25] J.A.G. Baggerman, R.J. Visser, E.J.H. Collart, *J. Appl. Phys.* 75 (2) (1994) 758–769.
- [26] A.G. Junior, F.G. Carlucci, D.M.G. Leite, W. Miyakawa, A.L.J. Pereira, M. Massi, A. S. da Silva Sobrinho, *Plasma nanotexturing of amorphous carbon films by reactive ion etching*, *Surf. Coat. Technol.* 354 (2018) 153–160.
- [27] H.J. Oswald, E. Turi, *Polym. Eng. Sci.* 5 (1965) 152.
- [28] A.D. Talley, B.R. Rogers, V. Iakovlev, R.F. Dunn, S.A. Guelcher, *J. Biomater. Sci. Polym. Ed.* 1 (2017).
- [29] A. Imel, T. Malmgren, M. Dadmun, S. Gido, J. Mays, *In vivo oxidative degradation of polypropylene pelvic mesh*, *Biomaterials* 73 (2015) 131–141.